



HAL
open science

Controlled and Chemoselective Hydrogenation of Nitrobenzene over Ru@C60 Catalysts

Faqiang Leng, I.C. Gerber, Pierre Lecante, Simona Moldovan, Maria Girleanu, M. Rosa Axet, Philippe Serp

► **To cite this version:**

Faqiang Leng, I.C. Gerber, Pierre Lecante, Simona Moldovan, Maria Girleanu, et al.. Controlled and Chemoselective Hydrogenation of Nitrobenzene over Ru@C60 Catalysts. ACS Catalysis, 2016, 6 (9), pp.6018-6024. 10.1021/acscatal.6b01429 . hal-01766217

HAL Id: hal-01766217

<https://hal.science/hal-01766217v1>

Submitted on 4 Feb 2025

HAL is a multi-disciplinary open access archive for the deposit and dissemination of scientific research documents, whether they are published or not. The documents may come from teaching and research institutions in France or abroad, or from public or private research centers.

L'archive ouverte pluridisciplinaire **HAL**, est destinée au dépôt et à la diffusion de documents scientifiques de niveau recherche, publiés ou non, émanant des établissements d'enseignement et de recherche français ou étrangers, des laboratoires publics ou privés.

Controlled and chemoselective hydrogenation of nitrobenzene over Ru@C₆₀ catalysts

Faqiang Leng,^{†,‡} Iann C. Gerber,[#] Pierre Lecante,[§] Simona Moldovan,[|] Maria Girleanu,^{|,⊥} M. Rosa Axet^{†,‡,*} and Philippe Serp^{†,‡,*}

[†] CNRS, LCC (Laboratoire de Chimie de Coordination), composante ENSIACET, 4 allée Emile Monso, BP 44099, F-31030 Toulouse Cedex 4, France

[‡] Université de Toulouse, UPS, INPT, F-31077 Toulouse Cedex 4, France

[#] Université de Toulouse; INSA, UPS, CNRS; LPCNO (IRSAMC), 135 avenue de Rangueil, F-31077 Toulouse, France

[§] CEMES-CNRS, 29 rue Jeanne Marvig, 31055 Toulouse Cedex 4, France.

[|] Institut de Physique et Chimie des Matériaux de Strasbourg, UMR 7504 CNRS-UdS, 23 rue du Loess BP43, 67034 Strasbourg cedex 2, France

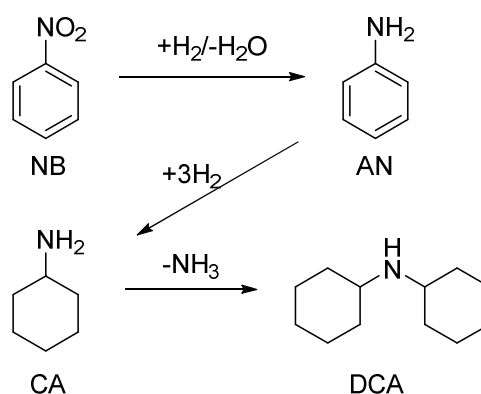
[⊥] Institut de Recherche Biomédicales des Armées, Unité Imagerie, Place du Médecin Général Inspecteur Valérie André, BP73, 91220 Brétigny-sur-Orge, France.

ABSTRACT: Electron deficient ruthenium nanoparticles supported on Ru fulleride nanospheres allows the successive and chemoselective hydrogenation of nitrobenzene, to aniline and then to cyclohexylamine. The catalysts were prepared in a straightforward manner by decomposition under dihydrogen of [Ru(COD)(COT)] in the presence of C₆₀. The nitrobenzene hydrogenation reaction is solvent sensitive, and proceeds faster in methanol than in other alcohols. The same behaviour, *i.e.* two steps successive hydrogenation, has been observed for several substituted nitroarenes. Density functional theory calculations suggest that the observed chemoselectivity is mainly governed by the presence of surface hydrides on the electron deficient Ru nanoparticles. At the threshold value of 1.5 H per Ru surface atom, the formation of aniline is favored due to the net preference of the NO₂-coordination.

KEYWORDS Ruthenium, C₆₀, fulleride, nitrobenzene hydrogenation, amine synthesis

Introduction

Selective hydrogenation is involved in many industrial processes, and it is one of the widest areas of research in catalysis. In particular, the catalytic hydrogenation of nitrobenzene (NB) is an industrially important reaction, which may lead to aniline (AN) or cyclohexyl amine (CA) as major products. Additionally, a condensation side reaction may produce dicyclohexylamine (DCA) as the major by-product (Scheme 1). It is admitted that in NB, the aromatic ring is electron deficient and coordinates only weakly to metals typically used in hydrogenation reactions. In contrast, the nitro group is strongly coordinating and is usually hydrogenated first. AN, which is an important intermediate for polyurethanes, dyes, pharmaceuticals, explosives, and agricultural products,¹ is industrially produced *via* NB selective hydrogenation. Reactions performed in the liquid phase used a variety of metal catalysts (Ni, Pt, and Pd) associated to modifiers, and organic solvents. For instance, DuPont hydrogenates NB in the liquid phase using a Pt-Pd catalyst on a carbon support with iron as modifier. The modifier provides good catalyst life, high activity, and protection against hydrogenation of the aromatic ring.¹ CA can be used in the synthesis of artificial sweeteners, metal corrosion inhibitors, rubber vulcanizing additives, dyestuff, plasticizers and extracting agents for natural products.²



Scheme 1. Main products and by-products formed during NB hydrogenation.

Commercially, it may be produced *via* reductive amination of cyclohexanol or phenol, or hydrogenation of AN. A variety of metals such as Ni, Co, Rh, Ru, Pd and Pt can be used for the hydrogenation of AN either in the vapor or in the liquid phase. The design of a single metal and non-promoted catalyst, which could hydrogenate in a controlled manner NB to produce selectively either AN, or CA in a single step is therefore of paramount interest. In this context, recent advances in the

design of nanostructured catalysts for selective hydrogenation have been recently reviewed.³ Supported ruthenium catalysts could be interesting candidates since the literature indicates that Ru is the best catalyst among the platinum metals for the hydrogenation of aromatic amines to alicyclic anilines,^{4,5} and in addition, a high selectivity towards AN can be obtained by careful choice of the support.^{6,7} Electron deficient Ru nanoparticles (NPs) have been reported to be highly active since AN desorption is facilitated.⁶ Furthermore, in the case of a controlled reaction, Ru could be more selective to AN, thanks to a preferential coordination of the nitro group. As far as the support is concerned, higher NB conversions have been reported when using carbon supports rather than silica or alumina.⁸ Carbon is rather chemically inert allowing avoiding condensation reactions, known for more acidic oxide supports. The direct reduction of NB to AN by carbon materials (carbocatalysis) such as fullerenes (C₆₀) or carbon nanotubes (CNTs) has also been discussed.⁹⁻¹¹ Ruthenium supported on CNTs allow for hydrogenation of both the aromatic ring and the nitro group,⁵ and CA was produced with 90% selectivity. In that case, the AN selectivity reached a maximum of 64%. The use of mixtures of CNT-supported Pt and Ru catalysts has also been proposed.¹² Indeed, mixtures of Pt/CNT, having a high activity in NB hydrogenation, and of Ru/CNT, highly selective for the hydrogenation of AN to CA, provided high activity at constant high selectivity. Ru/C-NaNO₂ catalyst was found to catalyze NB hydrogenation to produce AN (100% selectivity at 80°C) or CA (100% selectivity at 90°C) in high yield, depending on the reaction temperature.¹³ Considering the fact that C₆₀ is a well-known electron acceptor, a Ru@C₆₀ catalyst should provide electron deficient Ru NPs, which could be of interest for this reaction. Herein, we report a simple method for the preparation of Ru@C₆₀ catalysts consisting of a Ru fulleride core and a shell of C₆₀ stabilized Ru NPs. A significant charge transfer from ruthenium to fullerene has been evidenced by Raman spectrometry, XPS, and supported by density functional theory (DFT) investigations. These catalysts allow to obtain AN or CA with high selectivity (>90%) at 80°C under 30 bar of hydrogen.

Results and discussion

A series of Ru@C₆₀ catalyst with Ru/C₆₀ molar ratio ranging between 1 and 50 was prepared by decomposing [Ru(COD)(COT)] (COD = 1,5 cyclooctadiene, COT = 1,3,5-cyclooctatriene) under H₂ (3bar) in the presence of C₆₀ at r.t. in CH₂Cl₂ (see SI for experimental details). The decomposition reaction of [Ru(COD)(COT)] in the presence of C₆₀ results in the selective formation of spherical particles with mean diameter increasing with the Ru/C₆₀ ratio, from 36.2 ± 1.2 nm for Ru/C₆₀=1 (Figure 1-a) to 63.3 ± 0.8 nm for Ru/C₆₀=50. Depending on the Ru/C₆₀ ratio, these spherical particles can be or not surface decorated with metallic Ru NPs (< 1.5 nm). For a Ru/C₆₀ ratio of 1, a polymeric structure is obtained, in which each Ru atom is coordinated to two C₆₀, with a η²⁽⁶⁾-η⁶ coordination mode.¹⁴ HREM performed on this sample (Figure S1) did not reveal the presence of any Ru NPs. However STEM images (Figure 1-b) allow visualizing extremely small objects, isolated atoms and clusters with a few atoms that are stabilized on the surface of the Ru fulleride. They are seen as light gray dots distributed uniformly through the fulleride spheres.

This polymeric phase is the kinetic product of the reaction. The presence of isolated Ru atoms on the surface of these

spheres (single atom catalyst) should maximize the efficiency of metal atom use, which is particularly important for supported noble metal catalysts.¹⁵ For Ru/C₆₀ ratio > 1, Ru NPs are produced (Figure 1-c), presumably from the atom/cluster germs, producing the thermodynamic products of the reaction. The presence of Ru NPs only on the surface of the ruthenium fulleride has been confirmed by electron tomography (Figure 1-d,e). Interestingly, the Ru mean NP size does not change with the Ru loading (Table 1), and 1.35 ± 0.02 nm Ru NPs can be produced by this method for a Ru loading as high as 60% w/w.

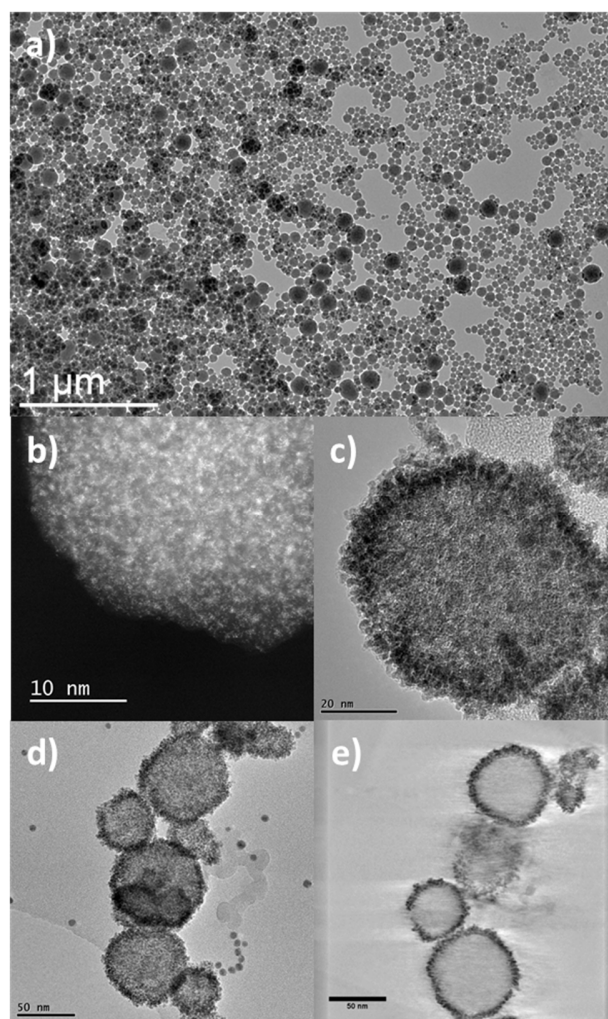


Figure 1. a) TEM micrograph of Ru@C₆₀ 1/1; b) STEM of Ru@C₆₀ 1/1 (scale bar 10 nm); c) HREM of Ru@C₆₀ 20/1 (scale bar 20 nm); d) and e) TEM and 3D analysis of Ru@C₆₀ 20/1 by electron tomography (scale bar 50 nm).

As XRD was not informative due to the very small size of the NPs, WAXS analyses have been undertaken. After corrections and Fourier Transforms, the related PDF functions are very close, and consistent with metallic Ru NPs with low structural disorder and sizes in the 1.5-2.5 nm range. From the shape of the envelope (Figure S2) characterized by a rapid initial decrease and a secondary maximum for a larger value (ca 1.5 nm) before the final decrease, size dispersion is likely, with a large proportion of NPs much smaller than the 2.5 nm value. This is in agreement with TEM measurements.

Table 1. Loading and mean particle size of the Ru@C₆₀ samples.

Ru/C ₆₀ ^a	Ru load ^b (%)	Ru NPs mean size (nm) ^c
1/1	10.6	Not observed
2/1	16.7	1.16 ± 0.02 nm
5/1	35.6	1.31 ± 0.03 nm
10/1	48.7	1.26 ± 0.03 nm
20/1	50.4	1.10 ± 0.01 nm
30/1	54.7	1.34 ± 0.01 nm
50/1	61.9	1.31 ± 0.02 nm

^a Synthesized by decomposing [Ru(COD)(COT)] under H₂ (3 bar) in the presence of C₆₀ at r.t. in CH₂Cl₂. ^b by ICP. ^c Manual measurement from enlarged TEM micrographs of at least 200 objects.

We independently checked that the decomposition of an excess of [Ru(COD)(COT)] (3 bar H₂, r.t., CH₂Cl₂) on the Ru@C₆₀ 1/1 sample, to reach a 10/1 ratio, does not produce the same material than Ru@C₆₀ 10/1 (Figure S3 for TEM). Indeed, while the Ru@C₆₀ 10/1 sample shows well dispersed Ru NPs on the fulleride spheres, the former sample shows the presence of aggregated Ru NPs deposited on the fulleride spheres. This is an indirect evidence of the fact that the C₆₀ should also contribute to the stabilization of the ruthenium NPs in the Ru@C₆₀ samples. DFT calculations performed on a Ru₁₃ cluster have shown a significant stabilization of the cluster upon C₆₀ coordination. Calculated cohesive energy per fullerene ranges between 64 and 92 kcal/mol for nC₆₀-Ru₁₃ (n=1-6) assemblies (see SI, Figure S4 and Table S1 for the computational details). The thermal stability of these nanostructures was evaluated by isothermal heating under argon. These structures are very stable up to 200°C, and begin to degrade at 400°C (Figure S5).

Significant charge transfer from ruthenium to fullerene has been evidenced by Raman spectrometry and XPS for all the prepared materials, which is an important factor to take into account, particularly if we consider the possible reactivity of these materials. Figure 2-a shows Raman spectra excited at 532 nm of C₆₀, Ru-C₆₀ 1/1, and 20/1 samples, in the spectral range of the tangential pitch mode A_g(2). It has been shown that the energy of the A_g(2) mode (1469.3 cm⁻¹ for pure C₆₀) is sensitive to charge transfer in transition metal fullerenes.¹⁶ We observe here a spectral shift as large as -8.7 cm⁻¹ for the Ru-C₆₀ 1/1 sample and -11.6 cm⁻¹ for the Ru-C₆₀ 20/1 samples well as, a significant broadening with increasing amount of C₆₀, caused by strong electron-phonon interaction. The charge transfer was also evidenced by XPS (Figure 2-b), by comparing the binding energy of Ru 3p_{3/2} in samples Ru-C₆₀ 1/1 and 20/1 with that of metallic ruthenium (461.2 eV): the measured binding energies were 462.2 and 461.5 eV for the

Ru-C₆₀ 1/1 and 20/1 samples, respectively. Theoretical charge transfers obtained by DFT for nC₆₀-Ru₁₃ (n=1-6) systems are ranging from 1.03 to 2.96 e⁻, for n=1 to n=6 respectively (Table S1).

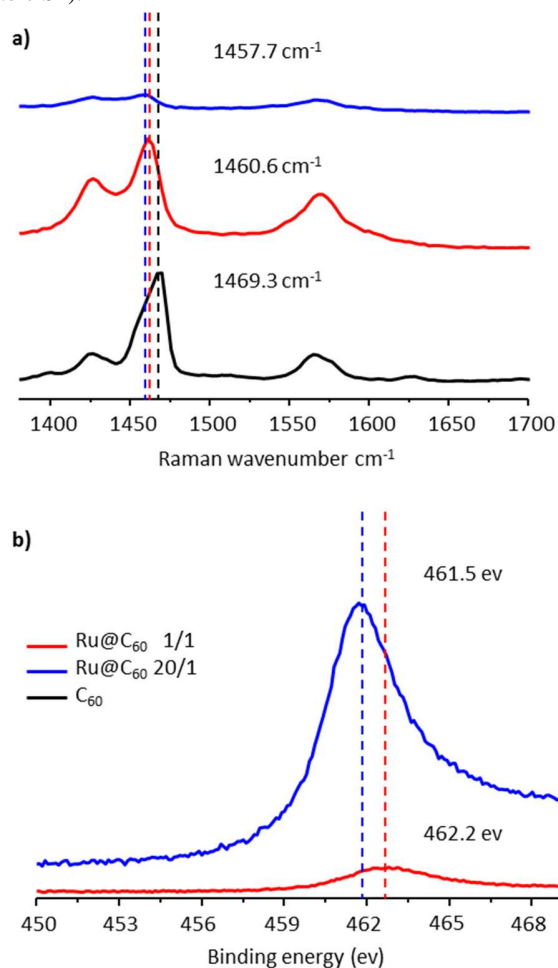


Figure 2. a) Raman spectra of excited at 532 nm of C₆₀ and Ru@C₆₀ 1/1 and 20/1 samples in the spectral range of the tangential pitch mode A_g(2); and b) XPS Ru 3p_{3/2} spectra of Ru@C₆₀ 1/1 and 20/1 samples.

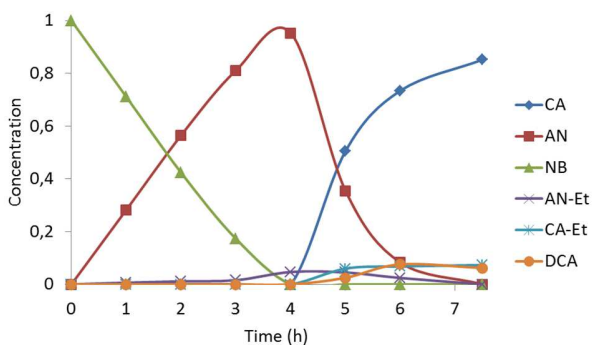
Nitrobenzene hydrogenation was studied at 30 bar H₂ and 80°C in ethanol. We independently checked that under these experimental conditions, C₆₀ has no activity for this reaction. Table 2 shows the results obtained with the Ru@C₆₀ samples at different Ru/C₆₀ ratio (see Figure S6 for the evolution of the conversion over the time). The main reaction products were AN and CA; DCA and N-ethylaniline (AN-Et), which is formed from N-alkylation of aniline due to reaction with the solvent,^{17,18} were the only detected by-products. All catalysts were found active for NB hydrogenation. The low loading catalysts (Ru/C₆₀ ratio < 5) were found inactive for the hydrogenation of the aromatic ring, and AN was produced with selectivity > 80%. This might be due to the extremely small size of the Ru NPs present in these samples, which might be poorly active for aromatic ring hydrogenation.^{19,20} At Ru/C₆₀ ratio ≥ 5, all catalysts were active for AN hydrogenation to CA. The remarkable feature of all these catalysts is that AN hydrogenation to CA starts only when complete NB hydrogenation to AN has been finished (see Figure 3 for the Ru@C₆₀ 10/1 catalyst).

Table 2. Results of hydrogenation of nitrobenzene in ethanol with different Ru@C₆₀ catalysts.

Ru/C ₆₀	Nitro- group		Selectivity [%] ^a		Aromatic ring		Selectivity [%] ^a		
	TOF h ^{-1b}	Time H	AN	AN-Et	TOF h ^{-1c}	Time h	CA	DCA	CA-Et
1/1	18.7	48	80	20	---	---	---	--	---
2/1	33.6	48	84	16	---	---	trace	--	---
5/1	44.3	24	96	4	132.2	6	91	4	5
10/1	55.7	4	90	10	100.4	3.5	86	7	7
20/1	60.8	3.5	91	9	182.1	2	84.5	8.5	7
30/1	59.8	3	91	9	123.1	1.5	82.5	9	8.5
50/1	42.6	3	92	8	134.5	1.5	89	5	6

Reaction conditions: 5 mg Ru@C₆₀ catalyst, 500 mg (4.06mmol) nitrobenzene, 200mg (1.1 mmol) dodecane (internal standard), 30 bar H₂, 80°C, 30 mL EtOH. ^a determined by GC-MS using internal standard technique. ^b TOFs calculated at 1h of reaction ($\approx 30\%$ of conversion) except for ratios 1/1 and 2/1 (3h). ^c TOFs calculated at 0.5h of reaction ($\approx 50\%$ of conversion) except for ratios 5/1 and 10/1 (1h).

To the best of our knowledge such behavior has never been reported before. Controlled and chemoselective hydrogenation of NB over these Ru@C₆₀ catalysts is thus possible. Indeed, selectivity towards AN higher than 90% and selectivity towards CA higher than 80% have been obtained whatever the Ru/C₆₀ loading. If we consider the activity of these catalysts, the TOF were systematically higher for the hydrogenation of the aromatic ring compared to the nitro group. Apparent activation energies for NB and AN hydrogenation for the Ru@C₆₀ 10/1 catalyst were calculated using the kinetics measured at 60, 80 and 90° C (5 mg of Ru@C₆₀ 10/1 catalyst, NB or AN 0.2M, 30 bar H₂, 20 mL EtOH see SI, Table S2 and Table S3 for further details). According to the NB and AN hydrogenation conversion rates in the temperature range of 60-90° C the calculated activation energies are 63.4 and 34.6 kJ/mol, respectively. Competitive hydrogenation in the presence of both NB and AN was performed using the Ru@C₆₀ 10/1 catalyst (see Table S4).

**Figure 3.** Time-concentration curve for NB hydrogenation with Ru@C₆₀ (Ru/C₆₀ = 10/1).

The reaction proceeds similarly, NB was selectively hydrogenated first with no presence of CA in the reaction mixture. The direct hydrogenation of AN also produced selectively CA, nevertheless the activity of the catalyst was lower (see Table S5). After reaction, the size of the Ru NPs, as well as the size of the Ru@C₆₀ nanospheres was not significantly changed (Table S6 and Table S7). Recyclability tests were performed with the Ru@C₆₀ 10/1 catalyst (see SI for experimental details and Table S8). A slight decrease of the final conversion was observed in the successive catalytic runs. Nevertheless, Ru was not detected in the final product by ICP analyses, indicating that there is no leaching of soluble Ru species. Taking into account these results, the decrease of the conversion during the recycling tests is more likely due to the slight increase of the Ru NPs mean size after catalysis (Table S6).

Highly exothermic reactions, such as NB hydrogenation often employ a solvent to help dissipating the excess heat generated during the reaction, and to prevent possible explosion. It has been shown that the nature of the solvent employed has a significant effect on the rate and selectivity of the catalytic hydrogenation reactions.²¹ Solvents may play different roles, in addition to the usual one (heat management, solubilisation), such as: i) change the solubility of hydrogen, ii) compete with the reactants for adsorption at the metal surface, iii) catalyze side reactions, iv) provoke catalyst agglomeration, and v) interact with the reactant. Concerning the latter effect, favorable thermodynamic interaction between the solvent and the reactant is expected to reduce the adsorption of the reactant on the catalyst, while unfavorable interaction should aid the adsorption. The Ru@C₆₀ 10/1 catalyst was used to evaluate the influence of the solvent (Table 3). Methanol, ethanol and isopropanol were compared. Hydrogen solubility in these solvent is expected to follow the order: iPrOH > EtOH > MeOH, as H₂ solubility in alcohols increases with the number

of carbon atoms.²² The relative permittivity (ϵ_r) follow the order MeOH ($\epsilon_r = 32.7$) > EtOH ($\epsilon_r = 24.5$) > iPrOH ($\epsilon_r = 17.9$). A significant solvent effect was noticed both on catalyst activity and selectivity. As far as the activity is concerned, methanol is by far the best solvent. Results obtained on Pd/C catalysts have shown that NB²³ or nitrotoluene²¹ hydrogenations proceed much more rapidly in methanol than in isopropanol or ethanol. It has been proposed that the interaction between the solvent and the reactant is probably the dominant factor that decides the overall effect of the

solvent on the rate of hydrogenation. The interactions seem to affect the energetics of the reaction, as reflected in the value of the activation energy, which was observed to change with the reaction medium.²¹ However, over palladium catalysts supported on nanodiamonds, the higher rates of NB hydrogenation were obtained in butanol, followed by ethanol and then methanol.²⁴

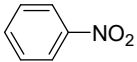
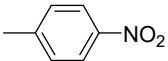
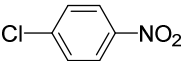
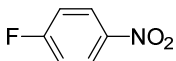
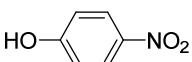
Finally, we also broadened the spectrum of substrates to substituted nitrobenzenes (Table 4), in order to vary the electron donating/withdrawing character of the substituent.

Table 3. Results of hydrogenation of nitrobenzene with the Ru@C₆₀ (Ru/C₆₀ = 10/1) catalyst in different solvents.

Solvent	Nitro- group		Selectivity [%] ^a		Aromatic ring		Selectivity [%] ^a		
	TOF h ^{-1b}	Time h	AN	N-alkylation	TOF h ^{-1c}	Time h	CA	DCA	N-alkylation
MeOH	42.6	3	98	2	134.5	3	88	5	7
EtOH	55.7	4	90	10	100.4	3.5	86	7	7
Isopropanol	37.0	6	100	0	45	4	94.5	2	3.5

Reaction conditions: 5 mg Ru/C₆₀ 10/1 catalyst, 500 mg (4.06mmol) nitrobenzene, 200mg (1.1 mmol) dodecane (internal standard), 30 bar H₂, 80°C, 30 mL solvent. ^a determined by GC-MS using internal standard technique. ^b TOFs calculated at 1h of reaction ($\approx 30\%$ of conversion). ^c TOFs calculated at 1h of reaction.

Table 4. Results of hydrogenation of substituted nitroarenes with the Ru@C₆₀ (Ru/C₆₀ = 10/1) catalyst in ethanol.

Substrate	Nitro- group		Selectivity [%] ^a		Aromatic ring		Selectivity [%] ^a		
	TOF h ^{-1b}	Time h	s-AN	N-alkylation	TOF h ^{-1b}	Time h	s-CA	s-DCA	N-alkylation
	55.7	4	90	10	100.4	3.5	86	7	7
	94.8	2.5	94	6	36.0	4.5	89	3.1	7.8
	109.3	2	92	8	38.6	5	96.7 ^c	1.5	1.8
	236.0	1	92.5	7.5	114.3	3	85.2 ^c	9.1	5.7
	168.4	1	98	2	24.3	7	87	n.d.	12

Reaction conditions: 5 mg Ru/C₆₀ 10/1 catalyst, (4.06mmol) nitroarene, 200mg (1.1 mmol) dodecane (internal standard), 30 bar H₂, 80°C, 30 mL solvent. ^a determined by GC-MS using internal standard technique at 100% conversion. ^b TOFs calculated at 1h of reaction. ^c Selectivity towards the de-halogenated substrate.

For all substrates tested, the stepwise hydrogenation to produce the fully hydrogenated amine was observed. As expected from the electronic effects, *p*-chloronitrobenzene and *p*-fluoronitrobenzene react faster than *p*-nitrotoluene to produce the respective aniline.²⁵ Further hydrogenation of toluidine, provides particular challenges with respect to chemo- and diastereoselectivity. Indeed: i) the aromatic ring can be fully or partially hydrogenated; ii) the amino group can be cleaved off or may be susceptible to parallel or consecutive reactions; and iii) the methyl group opens the possibility of *cis/trans* diastereomerism in the hydrogenated product. Paratoluidine was fully converted only after 4.5h. In parallel with the consumption of *p*-toluidine, *cis*- and *trans*-4-MCyNH₂ and small amounts of the three secondary amine (4-MCy)₂NH diastereomers were formed, as well as the N-alkylation product. *Cis*- and *trans*-4-MCyNH₂ were formed in a ratio of 4, which is unusually high for Ru/C catalysts.^{26,27} For chloro nitrobenzene hydrogenation, ruthenium is known as a good catalyst for minimizing dehalogenation, while keeping a fast rate for reduction of the nitro group.²⁸⁻³⁰ Chloroaniline is usually obtained with high selectivity on carbon supports.³¹⁻³³ The complete hydrogenation that should produce chlorocyclohexylamine has not been reported. However, it is known that on Pt/Al₂O₃ catalysts, after the hydrogenation of *p*-chloronitrobenzene to *p*-chloroaniline, the aromatic haloamine undergoes hydro-dechlorination to aniline, and further ring hydrogenation to cyclohexylamine.³⁴ After 2 hours of reaction the Ru@C₆₀ catalyst allows the production of *p*-chloroaniline with 92% selectivity. In a second stage, the *p*-chloroaniline undergoes hydro-dechlorination to AN, and further ring hydrogenation to produce CA. The *p*-fluoronitrobenzene shows the same behavior.

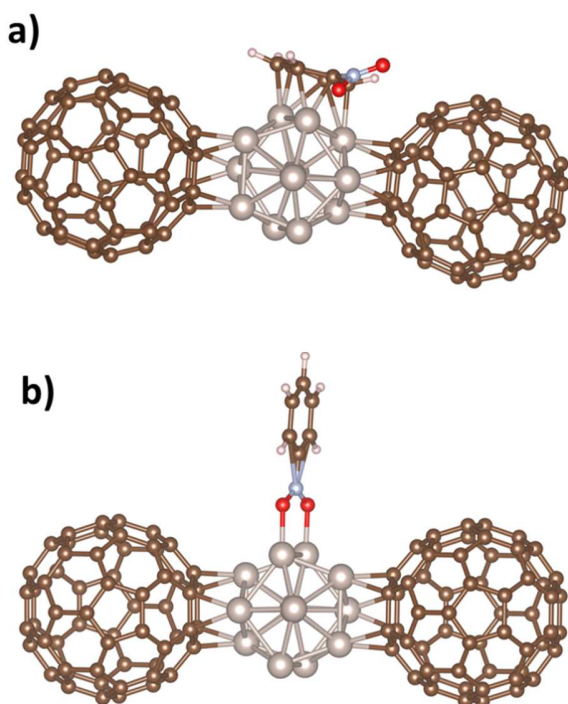


Figure 4. a) Side view of the π -mode coordination of a nitrobenzene molecule on a facet of a naked 2C₆₀-Ru₁₃ molecular complex; b) Side view of the NO₂-mode coordination of a nitrobenzene molecule on the edge of a naked 2C₆₀-Ru₁₃ molecular complex.

In order to understand the controlled and chemoselective hydrogenation of NB over the Ru@C₆₀ catalysts, a DFT study has been performed, in order to explore the coordination thermodynamics of a single NB molecule on a 2C₆₀-Ru₁₃ molecular model. Two coordination modes, denoted π -mode and nitro-mode, appeared to be in competition. The first mode is when the π -system of the NB interacts with a facet of the Ru₁₃. The second one corresponds to the nitro group attached to an edge of the cluster; see Figure 4a and 4b.

It is then clear that for the π -mode, both hydrogenation of the aromatic ring and the nitro group are possible, while only the latter will be available in the nitro-mode coordination. Without any hydrides on the metallic surface, the adsorption energy of both configurations is similar, -50 and -57 kcal/mol for nitro- and π -mode respectively. It has to be noted that for an infinite Ru(0001) surface, which could be viewed as a good approximation of facets presented by large Ru NPs,³⁵ the adsorption energy drops but remains in favor of the π -mode, -45 kcal/mol vs. -30 kcal/mol. This is an interesting result that is not in agreement with what is usually admitted.

Here we propose that the NO₂-mode is favored by the presence of numerous hydrides on the metallic surface, with an experimental ratio between 1.3 and 2 H per surface Ru atom.^{36,37} Recently a theoretical study has shown that on small Ru NPs, the maximum coverage value is 1.6 H per Ru surface atom.³⁸ As shown in Figure 5, for low coverage values, the π -mode is thermodynamically favored, but as soon as enough hydrides are present on the surface, the NO₂-mode becomes more stable. Considering the experimental conditions (temperature and pressure of H₂), it is possible to consider that the small metallic NPs are fully covered, and are preferential sites for the selective hydrogenation to aniline.

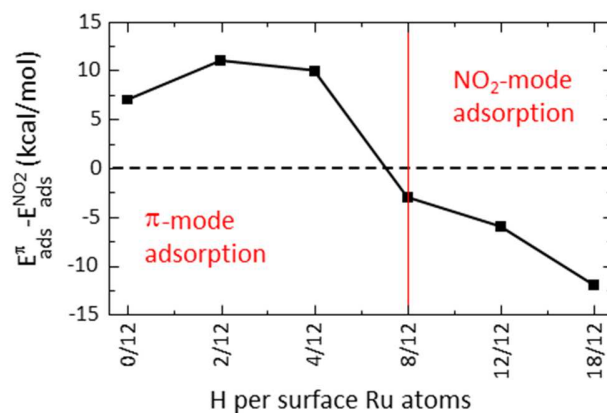


Figure 5. Evolution of the energy difference between the two adsorption modes with respect to the ratio of H per Ru surface atoms present on the metallic cluster.

Conclusion

We successfully prepared, in a straightforward manner, ruthenium@C₆₀ nano-objects. These structures consist in a ruthenium fulleride core (kinetic product of the reaction), surrounded by a shell of Ru NPs (\approx 1.5 nm). These materials are characterized by a significant charge transfer between Ru and C₆₀, providing electron deficient Ru centers. The catalytic activity of these objects has been investigated for NB hydrogenation. The remarkable feature of this study is the controlled and chemoselective hydrogenation of NB, which provides, first AN, and then CA, with high selectivities. DFT

calculations have shown that the coordination mode of NB on such nano-objects changes with the hydride coverage. At low coverage π -mode coordination is favored, for which both hydrogenation of the aromatic ring and the nitro group are possible. Whereas at high hydride coverage, NO₂-mode coordination prevails, for which only NO₂ hydrogenation is possible. Thus the combination of electron poor ruthenium nanoparticles and high hydride coverage explain the very high selectivity observed with Ru@C₆₀ catalysts. For comparison, a Ru/CNT catalyst gives only a maximum selectivity towards AN of 64%.⁵

ASSOCIATED CONTENT

Supporting Information.

The Supporting Information is available free of charge on the ACS Publications website at DOI:

Experimental section; TEM and HREM, WAXS, Raman, XPS characterization; kinetic data; complementary catalytic tests; recycling tests and additional DFT calculations. Figures S1–S8. Tables S1–S8. This material is available free of charge via the Internet at <http://pubs.acs.org>.

AUTHOR INFORMATION

Corresponding Author

*E-mail for P.S.: philippe.serp@ensiacet.fr

*E-mail for M.R.A.: rosa.axet@lcc-toulouse.fr

Notes

The authors declare no competing financial interest.

ACKNOWLEDGMENTS

This work was supported by the Centre National de la Recherche Scientifique (CNRS), which we gratefully acknowledge. The authors acknowledge financial support from the program of China Scholarships Council (CSC) for F. L. grant. I.C. Gerber also acknowledges the Calcul en Midi-Pyrénées initiative-CALMIP (Project p0812) for allocations of computer time.

REFERENCES

- (1) Kahl, T.; Schröder, K.-W.; Lawrence, F. R.; Marshall, W. J.; Höke, H.; Jäckh, R. In *Ullmann's Encyclopedia of Industrial Chemistry*; Wiley-VCH Verlag GmbH & Co. KGaA: 2011, p 465-478.
- (2) Roose, P.; Eller, K.; Henkes, E.; Rossbacher, R.; Höke, H. In *Ullmann's Encyclopedia of Industrial Chemistry*; Wiley-VCH Verlag GmbH & Co. KGaA: 2015, p 1-55.
- (3) Vilé, G.; Albani, D.; Almora-Barrios, N.; López, N.; Pérez-Ramírez, J. *ChemCatChem* **2016**, *8*, 21-33.
- (4) Greenfield, H. J. *Org. Chem.* **1964**, *29*, 3082-3084.
- (5) Tomkins, P.; Gebauer-Henke, E.; Leitner, W.; Müller, T. E. *ACS Catal.* **2015**, *5*, 203-209.
- (6) Komandur V. R. Chary, C. S. S. *Catal. Lett.* **2009**, *128*, 164-170.
- (7) Srikanth, C. S.; Kumar, V. P.; Viswanadham, B.; Srikanth, A.; Chary, K. V. R. *J. Nanosci. Nanotechnol.* **2015**, *15*, 5403-5409.
- (8) Zhao, F.; Zhang, R.; Chatterjee, M.; Ikushima, Y.; Arai, M. *Adv. Synth. Catal.* **2004**, *346*, 661-668.
- (9) Li, B.; Xu, Z. *J. Am. Chem. Soc.* **2009**, *131*, 16380-16382.
- (10) Niemeyer, J.; Erker, G. *ChemCatChem* **2010**, *2*, 499-500.
- (11) Wu, S.; Wen, G.; Wang, J.; Rong, J.; Zong, B.; Schlogl, R.; Su, D. S. *Catal. Sci. Technol.* **2014**, *4*, 4183-4187.
- (12) Tomkins, P.; Gebauer-Henke, E.; Müller, T. E. *ChemCatChem* **2016**, *8*, 546-550.
- (13) Oh, S. G.; Mishra, V.; Cho, J. K.; Kim, B.-J.; Kim, H. S.; Suh, Y.-W.; Lee, H.; Park, H. S.; Kim, Y. J. *Catal. Commun.* **2014**, *43*, 79-83.
- (14) Leng, F.; Gerber, I. C.; Lecante, P.; Bacsa, W.; Miller, J.; Gallagher, J. R.; Moldovan, S.; Girleanu, M.; Axet, M. R.; Serp, P. *RSC Advances* **2016**, DOI: 10.1039/C6RA12023G.
- (15) Yang, X.-F.; Wang, A.; Qiao, B.; Li, J.; Liu, J.; Zhang, T. *Acc. Chem. Res.* **2013**, *46*, 1740-1748.
- (16) Talyzin, A. V.; Jansson, U. *Thin Solid Films* **2003**, *429*, 96-101.
- (17) Li, X.; Zhang, J.; Xiang, Y.; Ma, L.; Zhang, Q.; Lu, C.; Wang, H.; Bai, Y. *Sci. China, Ser. B: Chem.* **2008**, *51*, 248-256.
- (18) Kim, J. W.; Yamaguchi, K.; Mizuno, N. *J. Catal.* **2009**, *263*, 205-208.
- (19) Pushkarev, V. V.; An, K.; Alayoglu, S.; Beaumont, S. K.; Somorjai, G. A. *J. Catal.* **2012**, *292*, 64-72.
- (20) Zhao, F.; Ikushima, Y.; Arai, M. *J. Catal.* **2004**, *224*, 479-483.
- (21) Rajadhyaksha, R. A.; Karwa, S. L. *Chem. Eng. Sci.* **1986**, *41*, 1765-1770.
- (22) d'Angelo, J. V. H.; Francesconi, A. Z. *J. Chem. Eng. Data* **2001**, *46*, 671-674.
- (23) Gelder, E. A.; Jackson, S. D.; Lok, C. M. *Catal. Lett.* **2002**, *84*, 205-208.
- (24) Obraztsova, I. I.; Eremenko, N. K.; Velyakina, Y. N. *Kinet. Catal.* **2008**, *49*, 401-406.
- (25) Sun, J.; Fu, Y.; He, G.; Sun, X.; Wang, X. *Catal. Sci. Technol.* **2014**, *4*, 1742-1748.
- (26) Gebauer-Henke, E.; Blumenthal, L.; Vogt, H.; Voss, G.; E., M. T. *ISJAE* **2010**, *84*, 29-36.
- (27) Gebauer-Henke, E.; Tomkins, P.; Leitner, W.; Müller, T. E. *ChemCatChem* **2014**, *6*, 2910-2917.
- (28) Tijani, A.; Coq, B.; Figueras, F. *Appl. Catal.* **1991**, *76*, 255-266.
- (29) Zuo, B.; Wang, Y.; Wang, Q.; Zhang, J.; Wu, N.; Peng, L.; Gui, L.; Wang, X.; Wang, R.; Yu, D. *J. Catal.* **2004**, *222*, 493-498.
- (30) Pietrowski, M.; Wojciechowska, M. *Catal. Today* **2009**, *142*, 211-214.
- (31) Oubenali, M.; Vanucci, G.; Machado, B.; Kacimi, M.; Ziyad, M.; Faria, J.; Raspolli-Galetti, A.; Serp, P. *ChemSusChem* **2011**, *4*, 950-956.
- (32) Antonetti, C.; Oubenali, M.; Raspolli Galletti, A. M.; Serp, P.; Vannucci, G. *Appl. Catal., A* **2012**, *421-422*, 99-107.
- (33) Bertolucci, E.; Bacsa, R.; Benyounes, A.; Raspolli-Galetti, A. M.; Axet, M. R.; Serp, P. *ChemCatChem* **2015**, *7*, 2971-2978.
- (34) Vitulli, G.; Verrazzani, A.; Pitzalis, E.; Salvadori, P.; Capannelli, G.; Martra, G. *Catal. Lett.* **1997**, *44*, 205-210.
- (35) Pan, C.; Pelzer, K.; Philippot, K.; Chaudret, B.; Dassenoy, F.; Lecante, P.; Casanove, M.-J. *J. Am. Chem. Soc.* **2001**, *123*, 7584-7593.
- (36) Garcia-Anton, J.; Axet, M. R.; Jansat, S.; Philippot, K.; Chaudret, B.; Pery, T.; Buntkowsky, G.; Limbach, H.-H. *Angew. Chem., Int. Ed.* **2008**, *47*, 2074-2078.
- (37) Berthoud, R.; Delichere, P.; Gajan, D.; Lukens, W.; Pelzer, K.; Basset, J.-M.; Candy, J.-P.; Coperet, C. *J. Catal.* **2008**, *260*, 387-391.
- (38) Cusinato, L.; Martinez-Prieto, L. M.; Chaudret, B.; del Rosal, I.; Poteau, R. *Nanoscale* **2016**, *8*, 10974-10992.

Insert Table of Contents artwork here

